TITLE: Fourier Transform THz-Wave Spectrometer Using THz-Wave Parametric Generator

Fourier Transform THz-Wave Spectrometer Using THz-Wave Parametric Generator

Jun-ichi Shikata, Kodo Kawase, Tetsuo Taniuchi, and Hiromasa Ito

Abstract—**We have developed a THz-wave spectrometer with the combination of a bright THz-wave source of THz-wave parametric generator (TPG) and a Martin-Puplett interferometer. The TPG output was optimized by studying various configurations with $LiNbO_3$ crystals. THz-waves which span the 1-2THz region were emitted with the peak power of 280μW. The whole system, including the nitrogen-purge unit, was constructed in a table-top size. By use of the THz-wave spectrometer, absorption lines of water vapor were successfully obtained.**

Index Terms—**terahertz-wave, parametric generator, nanosecond, arrayed Si-prism coupler, Fourier transform spectrometer, spectroscopy**

I. INTRODUCTION

There are increasing interests in experimental science and technology in the terahertz (THz)-wave region, where both generation and detection have been traditionally difficult. Recently, THz time-domain spectroscopy (THz-TDS) [1, 2] with a femtosecond laser attracted much attention, as the signal to noise ratio is much improved over that of conventional far-infrared Fourier transform spectrometers that use low-brightness incoherent sources and bolometric detectors. However, the conventional Fourier transform spectrometry, which directly measures the correlation of a THz-wave, has a vital importance as a standard method. In addition, considering the reflectivity measurements at the normal incident angle, it provides a simple and suitable experimental configuration [3]. Therefore, to improve S/N and to measure various samples with a large absorption, such as materials in biological tissues, the development of a compact and bright THz-wave source is essential.

In this paper, we describe the novel Fourier transform spectrometer, by combining a broad-band and bright source of THz-wave parametric generation (TPG) with a Martin-Puplett interferometer. The TPG is the single-pass version of the compact THz-wave parametric oscillator which we have studied [4-9]. Since THz-waves of a few-nanosecond pulsewidth are emitted, a long path difference of more than a few tens of centimeters and a high intensity are achieved. The first half of this paper is devoted to the optimization of the TPG output by studying various experimental configurations. Next, spectroscopic data measured with the spectrometer are demonstrated.

J. Shikata, T. Taniuchi, and H. Ito are affiliated with the Research Institute of Electrical Communication, Tohoku University, Sendai 980-8577, Japan.

K. Kawase is with Photo Dynamics Research Center, RIKEN, 519-1399 Aramaki Aoba, Aoba-ku, Sendai 980-0845, Japan.

H. Ito is also with Photo Dynamics Research Center, RIKEN.

II. PRINCIPLE OF THz-WAVE PARAMETRIC GENERATION

The efficient generation of THz-waves is based on the parametric scattering of laser light from the lowest A_1-symmetry polariton mode in $LiNbO_3$ (stimulated polariton scattering). The scattering process involves both second- and third-order nonlinear processes, thus a strong interaction occurs among the pump, idler and polariton (THz) waves. As shown in Fig. 1, polaritons exhibit photon-like behavior in the non-resonant frequency region, where a signal photon at THz frequency (ω_T) and a near-infrared idler photon (ω_i) are created parametrically from a near-infrared pump photon (ω_p), according to the energy conservation law $\omega_p=\omega_T+\omega_i$ (p: pump, T: THz, i: idler). In the stimulated scattering process, the momentum conservation law $\boldsymbol{k}_p = \boldsymbol{k}_i + \boldsymbol{k}_T$ (noncollinear phase-matching condition; see the insets of Fig.1) also holds. This leads to the angle-dispersive characteristics of the idler and THz-waves generated.

In spite of the efficient parametric interaction, most of the THz-wave generated is absorbed or totally reflected inside the $LiNbO_3$ crystal. This is due to the heavy absorption loss (more than several tens cm^{-1}) and the large refractive index (>5) in the THz range. To overcome the problem, we have proposed the Si-prism-output-coupler method [5], as shown in Fig. 2. Since the absorption

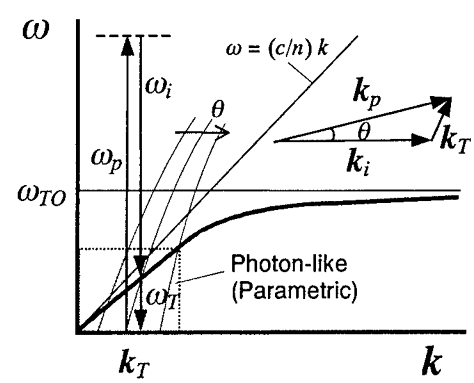

Fig. 1. Dispersion relation of the polariton, an elementary excitation generated by the combination of a photon and a transverse optical phonon (ω_{TO}). The inset shows the noncollinear phase-matching condition.

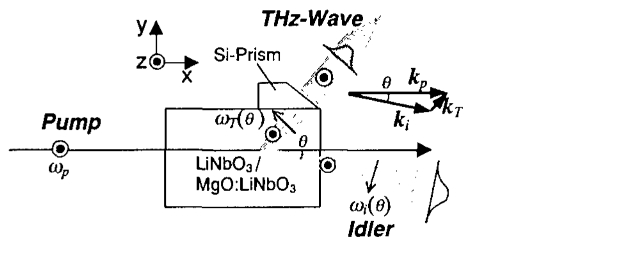

Fig. 2. Schematic diagram of single-pass THz-wave parametric generation (TPG) using a Si-prism-output coupler.

coefficient of Si is small ($\sim$0.6cm^{-1}) and the refractive index is almost fixed to be 3.4 in the THz region, a THz-wave beam with a low divergence (less than a few degrees) is efficiently coupled out via Si-prism according to Snell's law.

III. OPTIMIZATION OF TPG OUTPUT

In order to obtain a stable high power THz-wave output, the single-pass TPG was studied with various configurations of $LiNbO_3$ crystals. The experimental setup is shown in Fig. 3. The pump source was a Q-switched Nd:YAG laser (New Wave MiniLase II, wavelength: 1.064μm, pulse width: 7ns, typical output: 16mJ/pulse, spot size: 1mm), polarized along the z-axis of the crystal. 65mm-long undoped $LiNbO_3$ (LN) and 5mol% MgO:$LiNbO_3$ (MgO:LN) crystals [8] were used to generate THz-waves, and the end-surfaces of the crystals were anti-reflection coated for operation at around 1.07μm. The pump path was set very close to the Y-surface of the crystal to reduce the absorption loss of THz-waves. An array of THz-wave output couplers [9] consisting of six Si-prisms fabricated from a high resistivity Si crystal (ρ>1kΩ, $\alpha \cong$0.6cm^{-1}, total base length: 51mm) was introduced to obtain a high THz output. The angle of each prism was chosen as 39 degrees such that THz-waves were emitted almost normal to the prism surface. To obtain a high gain and a low threshold within the limitation of each crystal length (65mm), the crystals were arrayed in series along the x-axis with the prism coupler at the exit of the pump path (Fig. 3). The emitted THz-wave and near-infrared idler (Stokes) wave were measured with a 4 K Si-bolometer and a pyroelectric detector, respectively.

Optimization began with an examination of the gap between two LN crystals, as this will cause the decrease in the TPG output, due to the decrease in the interaction volume between the pump and the idler under the noncollinear phase-matching condition. As shown in Fig. 4, there was a monotonic decrease in the TPG output, but the power remains almost unchanged with the gap to around 5mm. In the experiment shown below, the gap of around 0.5mm was chosen.

Next, the input-output characteristics of the TPG-idler wave were studied. With the increase of the total crystal length, a monotonic increase in the idler output and a the monotonic decrease in the generation threshold were achieved, as shown in Fig. 5. It was also noted that MgO:LN [8] exhibited a better performance than undoped crystal. However, the THz-wave output did not correspond with the results of the idler, as shown in Fig. 6. Although the generation threshold decreased with the crystal length, the THz-wave power was saturated at the pump level of less than 16mJ when more than two crystals were used. The maximum THz-wave power and the highest stability was

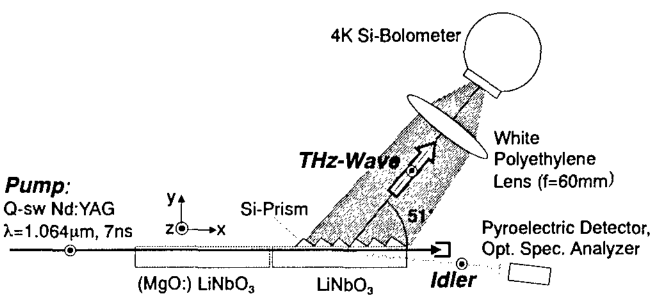

Fig. 3. Experimental setup for measuring TPG output

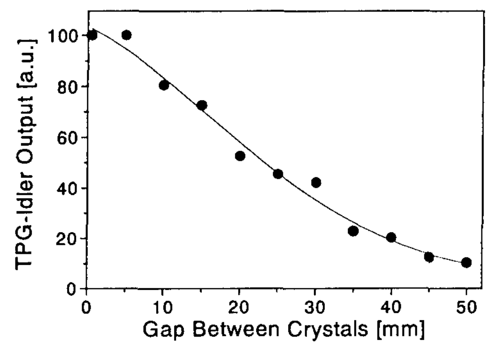

Fig. 4. Power dependence on the gap between two $LiNbO_3$ crystals.

Crystal(s)	Single Prism	Arrayed Prism	Enhancement Factor
LN (L=65mm)	0.8 μW	15.2 μW	× 19
LN×2 (L=130mm)	1.4	**272.8**	**×195**
LN+MgO:LN (L=130mm)	1.4	**279.2**	**×199**
LN×3 (L=195mm)	1.9	224.0	×118
LN+MgO:LN×2 (L=195mm)	2.2	104.0	× 47

Table 1. TPG-THz-wave output for various configuration (L: total crystal length, pump energy: 15.9 mJ).

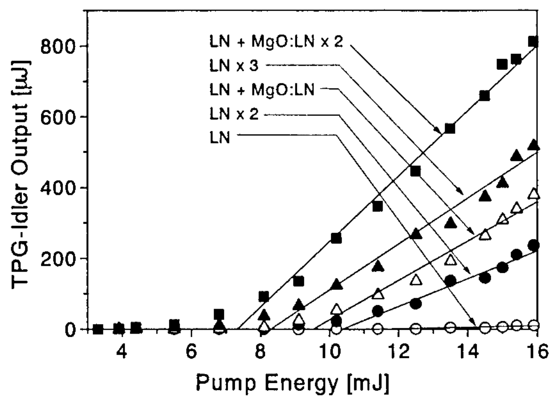

Fig. 5. Input-output characteristics of TPG-idler using LN and MgO:LN crystals.

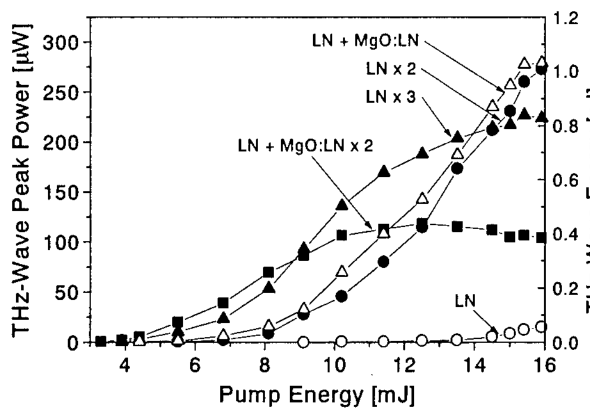

Fig. 6. Input-output characteristics of TPG-THz-wave using LN and MgO:LN crystals

achieved by use of two crystals at a pump energy of 15.9 mJ (conversion efficiency~5×10^{-11}). A comparison of the TPG THz-wave output with a single Si-prism output coupler (base length: 15mm) was also examined (Table 1). Power enhancement of more than two orders was obtained by introducing the arrayed Si-prism coupler.

To study further the saturation mechanism and the bandwidth of the THz-wave generated inside LN, the idler spectrum of two LN crystals was measured with an optical spectrum analyzer. The spectrum (frequency shift) extended from 30 to 120 cm^{-1} (0.9-3.6 THz), as shown in Fig. 7. The dip at 1.0696μm corresponds to the frequency shift of $47cm^{-1}$, and therefore the spectral component around 1.075μm (frequency shift: $94cm^{-1}$) represented the second Stokes component. Alternatively, low frequency resonances in $LiNbO_3$ were reported at 1.3THz ($=43cm^{-1}$) and 2.4THz ($=80cm^{-1}$) from the impulsive-response measurement [10]. However, these levels were slightly different from the dip position in our data (47, $75cm^{-1}$), and the linewidths were narrower. In particular, the Stokes component should not decrease with the resonance levels. Thus, this process was not dominant in our experiment.

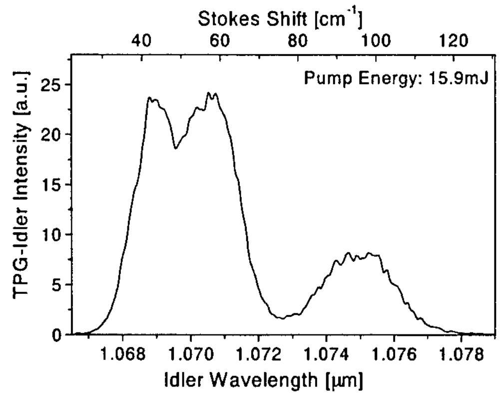

Fig. 7. Spectrum of TPG-idler generated with two $LiNbO_3$ crystals.

IV. APPLICATION TO SPECTROSCOPY

Using the optimized TPG source with two $LiNbO_3$ crystals and an arrayed Si-prism coupler, a Martin-Puplett THz-wave spectrometer was developed in a table top size (Fig. 8). With the advantage of linear polarization characteristics of TPG, the interferometer simply requires two wire grid polarizers. In order to collimate the THz-wave beam, an aperture and an off-axis parabolic mirror were used. The linear stage has a maximum stroke of 20cm, and therefore a resolution of $0.025cm^{-1}$ (=750MHz) is possible. LabVIEW software was used to control the system.

Fig. 9 shows an example of interferograms measured with the purge of nitrogen, and the power spectrum obtained from the Fourier transform is shown in Fig. 10. In this experiment, the maximum path difference was 50mm, which corresponds to a resolution of $0.1cm^{-1}$. The dip positions in the spectrum were in good agreement with the absorption lines of water vapor [11]. The TPG-THz-wave output corresponded to the first-order Stokes component. To obtain the high frequency component of THz-wave (~ $100cm^{-1}$), further techniques to reduce the absorption loss in $LiNbO_3$ are required, which will be achieved by

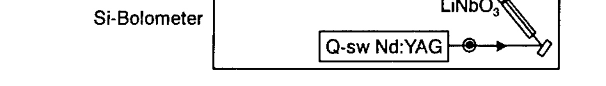

Fig. 8. Schematic diagram of a Fourier transform THz-wave spectrometer, combining a TPG-THz waves generator and a Martin-Puplett interferometer.

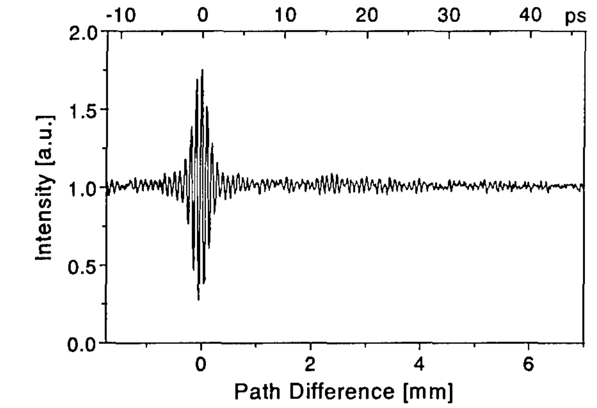

Fig. 9. Measured interferogram of TPG THz-wave in the nitrogen-purge unit.

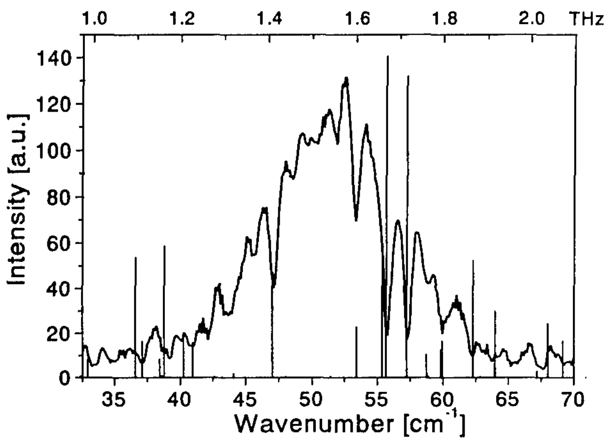

Fig. 10. TPG THz-wave spectrum obtained from the data shown in fig. 9, and the resolution is 0.1cm^{-1}. The absorption lines of water vapor are also indicated.

minimizing the propagation distance of the THz-wave using the total reflection of both the pump and the idler beam [7], or by cooling the crystal [6].

V. SUMMARY

We have described the characteristics of broad-band TPG-THz-wave generation, and its application in a Fourier transform spectrometer. This compact interferometer with bright source will be a powerful tool for spectroscopic studies of various materials in the THz region, such as solid state materials with strong absorption, biological tissues, and so on.

Acknowledgments

The authors are greatly indebted to C. Takyu and T. Shoji for their excellent work in coating and polishing. This work has been partly supported by the Grant-in Aid from the Ministry of Education, Science and Culture of Japan. Also, J. S. is supported by the Murata Science Foundation in Japan.

References

[1] D. M. Mittleman, R. H. Jacobsen, and M. C. Nuss, "T-ray imaging," IEEE J. Selected Topics in Quantum Electron., vol. 2, pp. 679-691, 1996, and references there in.

[2] P. Y. Han, X.-C. Zhang, "Coherent, broadband midinfrared terahertz beam sensors," Appl. Phys. Lett., vol. 73, pp. 3049-3051, 1998.

[3] D. H. Martin, "Polarizing (Martin-Puplett) Interferometric Spectrometers for the Near- and Submillimeter Spectra," in Infrared and Millimeter Waves, vol. 6., Chapter 2, 1982.

[4] K. Kawase, M. Sato, T. Taniuchi, and H. Ito, "Coherent tunable THz-wave generation from $LiNbO_3$ with monolithic grating coupler," Appl. Phys. Lett. vol. 68, pp. 2483-2485, 1996.

[5] K. Kawase, M. Sato, K. Nakamura, T. Taniuchi, and H. Ito, "Unidirectional radiation of widely tunable THz-wave using a prism coupler under noncollinear phase matching condition," Appl. Phys. Lett., vol. 71, pp. 753-755, 1997.

[6] J. Shikata, M. Sato, T. Taniuchi, H. Ito, and K. Kawase, "Enhancement of terahertz-wave output from $LiNbO_3$ optical parametric oscillators by cryogenic cooling," Opt. Lett., vol. 24, pp. 202-204, 1999.

[7] A. Morikawa, K. Kawase, J. Shikata, T. Taniuchi, and H. Ito, Optical parametric THz-wave generation using trapezoidal $LiNbO_3$," Proc. SPIE, vol. 3828, pp. 302-310, 1999.

[8] J. Shikata, K. Kawase, K. Karino, T. Taniuchi, and H. Ito, "Tunable terahertz-wave parametric oscillators using $LiNbO_3$ and MgO:$LiNbO_3$," IEEE Trans. MTT, vol. 48, pp. 653-661, 2000.

[9] K. Kawase, J. Shikata, H. Minamide, K. Imai, and H. Ito, "Arrayed silicon prism coupler for a THz-wave parametric oscillator," submitted to Applied Optics.

[10] H. J. Bakker, S. Hunsche, and H. Kurz, "Investigation of anharmonic lattice vibrations with coherent phonon polaritons," Phys. Rev. B, vol. 50, pp. 914-920, 1994.

[11] H. M. Pickett, R. L. Poynter, E. A. Cohen, M. L. Delitsky, J. C. Pearson, H. S. P. Muller, "Submillimeter, Millimeter, and Microwave Spectral Line Catalog," JPL Publication 80-23, Rev. 4, NASA, 1996; also, http://spec.jpl.nasa.gov.